CAVITY BPM DESIGNS, RELATED ELECTRONICS AND MEASURED PERFORMANCES

D. Lipka*, DESY, Hamburg, Germany

Abstract

Future accelerators like the International Linear Collider and Free-Electron Lasers require beam position measurements with submicron resolution in critical parts of the machines. This is achievable using the Cavity Beam Position Monitors (BPM). This paper presents the basic principles of this monitor type. Different institutes are working on the design of cavity BPM systems. An overview of recent developments with results and limitations is given.

INTRODUCTION

The international linear collider (ILC) will require high performance beam position monitors (BPM) to control the beam trajectory with high precision in order to maintain a stable collision of nanometer sized beams. The BPMs have to be located at specific positions along the linac up to the interaction point, where a few nanometer resolution is required. Additionally a spectrometer will be used in order to measure the beam energy. The spatial beam offset corresponds directly to the beam energy. To minimize the influence to the emittance the offset has to be small, therefore high precision BPMs are required for the ILC spectrometer with a resolution of 500 nm or better [1].

In case of Free-Electron Lasers (FEL) the overlap of the electron beam with the photon beam along the undulators less than 10 % of the transverse size is required. Typical transverse sizes of beams are of the order of 30 μm. Therefore a resolution better than 1 μm is required.

In comparison to other types of BPMs, like e.g. the button [2] or stripline [3] BPM, only the cavity BPM has the potential to achieve such high resolutions on a bunch by bunch time-scale. In this paper the cavity BPM principle is discussed, followed by the description of the electronics, resolution limitations and measurement methods. A few examples of such BPMs are presented.

THEORY OF CYLINDRICAL CAVITY BPMS

Electric Fields

The electric field $\mathbf{E}$ of a cavity can be derived from the d'Alembert equation

$$\Delta \mathbf{E} - \frac{1}{c^2}\frac{\delta^2 \mathbf{E}}{\delta t^2} = 0 \tag{1}$$

with c being the speed of light. For a cavity with radius R and length L only the z component is of interest. The

* dirk.lipka@desy.de

02 BPMs and Beam Stability

solution can be represented as

$$E_{z,mnp}(r,\phi,z,t) = CJ_m\left(\frac{j_{mn}r}{R}\right)\cos{(m\phi)}e^{-i\left(\omega_{mnp}t \mp \frac{p\pi z}{L}\right)}. \tag{2}$$

Here j_{mn} denotes the n-th zero of the Bessel function J_m of order m and

$$\omega_{mnp} = c\sqrt{\left(\frac{j_{mn}}{R}\right)^2 + \left(\frac{p\pi}{L}\right)^2} \tag{3}$$

is the angular resonant frequency of the mode mnp. The two first modes have $j_{01} = 2.405$ and $j_{11} = 3.832$ [4]. The first mode (monopole mode, TM$_{010}$) does not depend on the spatial component ϕ, therefore a cylinder symmetric mode is generated, as shown in Fig. 1. The Bessel func-
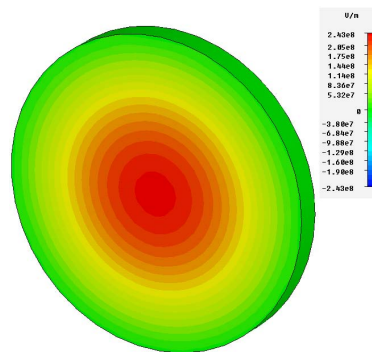

Figure 1: Field distribution of the first monopole mode in a cylindrical resonator. Simulation [5] is used.

tion of the order $m = 0$ does not depend of the radius r close to the cavity center. Therefore the field strength is proportional to the beam charge. The second mode (dipole mode, TM$_{110}$) depends on ϕ resulting in a field distribution as shown in Fig. 2. For a beam passing close to the cavity center the Bessel function of order $m = 1$ can be derived proportional to r. For that reason the field strength is proportional to the beam offset and charge.

Nowadays cylindrical cavities can be produced with very high accuracy. Therefore by measuring the field strength of the dipole mode a high resolution of the position information can be obtained.

Line Voltage

The normalized shunt impedance

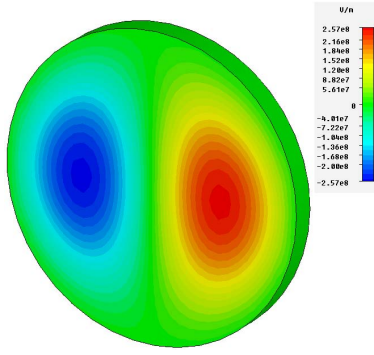$$\frac{R}{Q} = \frac{V^2}{\omega W} \tag{4}$$

Figure 2: Field distribution of the first dipole mode in a cylindrical resonator (horizontal orientation), a second dipole mode with vertical orientation and the same resonance frequency is generated as well, not shown here. Simulation [5] is used.

characterizes the energy exchange between the beam and the cavity. Here W is the energy stored in the cavity and

$$V = \left| \int_0^L E_z dz \right|. \tag{5}$$

The integration path goes along the particle trajectory. It is convenient to define a shunt impedance $(R/Q)_0$ at a certain offset x_0 with respect to the electrical center of the cavity for the dipole mode

$$\frac{R}{Q} = \left(\frac{R}{Q}\right)_0 \frac{x^2}{x_0^2}. \tag{6}$$

The energy after passing a longitudinally Gaussian-like distributed bunch with a length σ_z and a charge q is given by [6]

$$W = \frac{\omega}{4} \left(\frac{R}{Q}\right)_0 \frac{x^2}{x_0^2} q^2 \exp\left(-\frac{\omega^2 \sigma_z^2}{c^2}\right). \tag{7}$$

Only a fraction of the energy will be coupled out of the cavity depending on the external quality factor

$$Q_{ext} = \frac{\omega W}{P_{out}}. \tag{8}$$

Taking into account an output line with impedance Z the voltage is

$$V_{out} = \sqrt{ZP_{out}} = \sqrt{Z \frac{\omega W}{Q_{ext}}}$$
$$= \frac{\omega}{2} \sqrt{\left[\frac{Z}{Q_{ext}} \left(\frac{R}{Q}\right)_0\right]} q \frac{x}{x_0} \exp\left(-\frac{\omega^2 \sigma_z^2}{2c^2}\right). \tag{9}$$

The fraction $V_{out}/(qx)$ defines the sensitivity of the BPM.

The power dissipated in the cavity wall can be described by the internal quality factor Q_0

$$P_{diss} = \frac{\omega W}{Q_0}. \tag{10}$$

02 BPMs and Beam Stability

By combining both quality factors the loaded quality factor is

$$\frac{1}{Q_L} = \frac{1}{Q_0} + \frac{1}{Q_{ext}}. \tag{11}$$

The energy stored in the cavity decays proportional to the loaded quality factor

$$\tau = \frac{2Q_L}{\omega}. \tag{12}$$

For a single bunch measurement the signal should decay faster compared to the bunch spacing.

The line voltage parallel to the cavity axis results in

$$V_x(t) = V_{out} e^{-\frac{t}{\tau}} \sin(\omega t). \tag{13}$$

Note: There are two definitions of τ, the other is without factor 2 in (12), in this case the factor 2 has to be added in the denominator of the exponential in the equation (13).

The amplitude V_{out} depends on the product of beam offset and beam charge, therefore by measuring the amplitude and charge separately the offset can be obtained. The charge can be measured from the amplitude of a monopole mode. In most cases a second (reference) resonator tuned to the TM_{010} mode is used, also giving the relative phase between the dipole and the monopole mode and thus the direction of the beam offset.

Influence of the Beam Angle

If a beam enters the cavity under an angle α, each half of the resonator induces an offset with $\pm\alpha L/4$, see Fig. 3. The induced field is a dipole mode. The timing oscillation
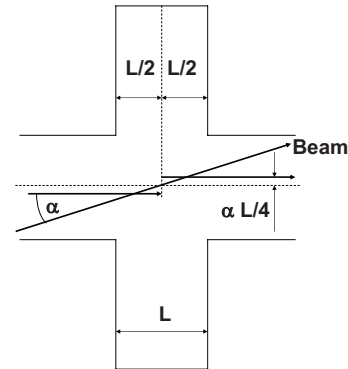

Figure 3: Sketch for the influence of the beam angle α.

in the equation (13) can be divided in each half of the resonator. The measured voltage is then

$$V_\alpha = C^* \left[\sin(\omega(t + L/4c)) - \sin(\omega(t - L/4c))\right]$$
$$= 2C^* \sin\left(\frac{\omega L}{4c}\right) \cos(\omega t). \tag{14}$$

Note that the oscillation caused by a beam angle is shifted by 90° with respect to the signal caused by an offset. The fraction of the angle influence to the offset signal x is about $\omega L^2 \alpha/(8\sqrt{2}cx)$. For short cavities the influence of the beam angle is reduced.

Influence of the Bunch Tilt

Consider a bunch with a tilt Θ with respect to the cavity axis, as shown in Fig. 4. In this case the bunch can be
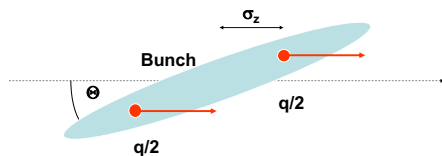

Figure 4: Sketch for the influence of the bunch tilt Θ.

divided into two parts each carrying a half of the bunch charge and contributing to the dipole mode. The measured voltage from the BPM in this case is:

$$V_\Theta = C^{**}\left[\sin\left(\omega(t+\sigma_z/c)\right) - \sin\left(\omega(t-\sigma_z/c)\right)\right]$$
$$= 2C^{**}\sin\left(\frac{\omega\sigma_z}{c}\right)\cos\left(\omega t\right). \tag{15}$$

The signal is shifted by $90°$ with respect to the offset signal. The fraction of the tilt influence to the offset signal is about $\Theta\omega\sigma_z^2/(2cx)$. A shorter bunch will have less effect to the dipole mode.

Rejection the Monopole Mode

The resonance frequency of the monopole mode is different of that of the dipole mode but the amplitude of the monopole mode is orders of magnitude larger compared to the dipole mode. Furthermore, at a moderate loaded quality factor there is a contribution at the dipole mode frequency due to the given bandwidth of the monopole mode.

Therefore a spatial filter (a slot or a waveguide) has to be inserted on the resonator, as described in ref. [7]. Usage of the slot exploits the differences in the field distribution of the monopole and dipole modes in order to reject the tails from the monopole mode, as shown in Fig. 5. The monopole mode is damped in the slot but the dipole mode can still propagate. By inserting an antenna in the waveguide/slot the voltage of the dipole can be measured like represented in the equation (13).

Waveguides provide a larger orthogonal coupling reduction compared to antennas mounted directly in the cavity. One has to point out that the waveguides/slots have to be implemented with high precision. Otherwise it would shift the dipole mode distribution resulting in higher orthogonal coupling [9].

ELECTRONICS

The signal processing can be done as shown in Fig. 6. In a hybrid the two opposite signals (which have a phase shift of $180°$) are subtracted. This reduces the influence of the monopole mode and doubles the amplitude of the dipole mode. Due to different cable length the phase of $180°$ can be shifted. Therefore phase shifters are connected before the hybrid to compensate the shift. In some cases the amplitude from the rejection of dipole and monopole modes
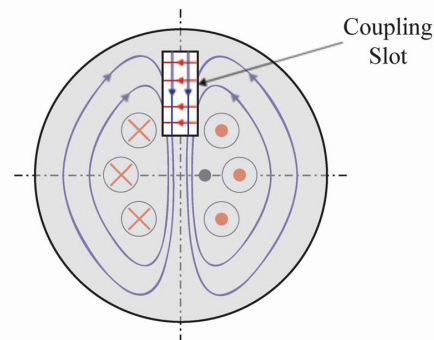
02 BPMs and Beam Stability

Figure 5: The dipole mode is selectively coupled out by means of two long, narrow, radial slots on one cavity face. The beam is indicated by a black dot, the electric field vector points circumferentially across the slot while the magnetic field vector points radially. The cavity has four slots (two for each plane to assure the symmetry). Details are given in ref. [8]
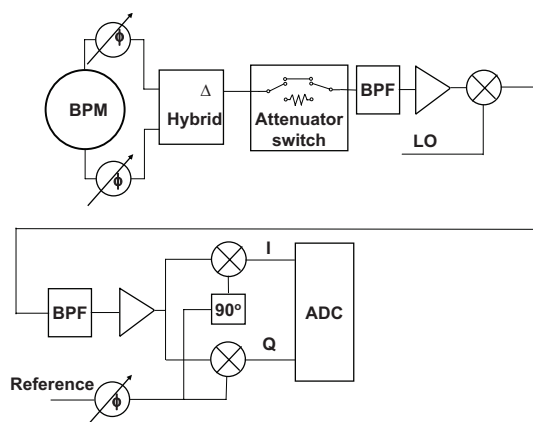

Figure 6: Block diagram of the electronics used for the signal processing of the dipole resonator.

due to spatial filter is large enough to dispense this part. This scheme is less sensitive to phase drifts due to temperature changes. To increase the dynamic range a switchable attenuator can be integrated in the electronics. A band-pass filter rejects higher order modes and an amplifier increases the amplitude.

If the following electronics can not be positioned close to the BPM, the signal has to be transmitted via long cables. The transmission of high frequency signals via cables is low, therefore down conversion with a local oscillator (LO) is done to an intermediate frequency. Two frequencies are multiplied:

$$A\sin\left(\omega_1 t+\phi_1\right)\cdot B\sin\left(\omega_2+\phi_2\right)=$$
$$\frac{AB}{2}[\cos\left((\omega_1-\omega_2)t+(\phi_1-\phi_2)\right)- \tag{16}$$
$$\cos\left((\omega_1+\omega_2)t+(\phi_1+\phi_2)\right)].$$

Followed by a low-pass filter only the lower frequency $\omega_1-\omega_2$ is received.

The intermediate frequency can be transported with lower attenuation to the other part of the electronics. Here a second band-pass filter for the intermediate frequency is used followed by an amplifier. Two parallel down conversions (I-Q demodulation) are used with a reference frequency either with a matched phase (realized with the phase shifter beforehand) and with reference frequency shifted by $90°$. This reduces the influence of beam angle α and bunch tilt Θ, compare with equations (13), (14) and (15).

Two methods are in use for the I-Q demodulation: Homodyne and Heterodyne one. The first one uses the same frequency as the dipole mode. Therefore the same intermediate frequency enters the conversion. This results in a zero frequency, as follows from equation (16) and only the amplitude information is maintained. The Heterodyne method uses a reference frequency, which is different from the intermediate frequency. In this case a lower frequency provides the amplitude and phase information.

The used electronics can imply all components mentioned above as shown in Fig. 6, but some of those can be dispense. For example the remote controlled attenuation switch is used only when a large dynamic range is required, or the first down conversion is used only if the I-Q demodulator is positioned far away from the BPM. In case the resolution above $1\,\mu$m is required, the I-Q demodulation is not in use.

RESOLUTION

The position signal is influenced by the monopole signal, by the beam angle and bunch tilt, by orthogonal coupling and cavity noise. The latter can be calculated as

$$V_{noise} = \sqrt{4kTZBW}, \quad (17)$$

where k is the Boltzmann constant, T is the temperature, Z is the impedance (usually $50\,\Omega$) and BW is the bandwidth of the entire system including the electronics. The amplifiers of the electronics will amplify also the cavity BPM noise. Additional electronics noise will contribute, degrading the resolution. The amplifiers and the ADC usually have the largest contributions to the noise. Therefore low noise components for the electronics with stabilized environment temperature have to be chosen.

MEASUREMENTS

The resolution of a cavity BPM is measured by using 3 BPMs placed one after another with distances $z_{ij} = z_i - z_j$ $(i, j = 1, 2, 3)$ to exclude the beam jitter. The outer BPMs (1,3) are measuring the beam position and predict the position on the BPM 2. The difference of several measurements gives the RMS value σ_2. For the resolution R_2 a geometric factor has to be taken into account as described in ref. [6]

$$R_2 = \frac{\sigma_2}{\sqrt{1^2 + \left(\frac{z_{12}}{z_{13}}\right)^2 + \left(\frac{z_{23}}{z_{13}}\right)^2}}. \quad (18)$$

Here one has to assume that all three BPM have the same resolution. For $z_{13}/2 = z_{12} = z_{23}$ the equation (18) simplifies to $R_2 = \sigma_2\sqrt{2/3}$.

Another method for the resolution measurement is the correlation of a large number of BPMs with a single BPM of a long beamline. In this case the resolution will be overestimated because the other BPMs are assumed to be noise free.

EXAMPLES OF RECENT MEASUREMENTS

SPring-8 Compact SASE Source Cavity BPM Prototype

The design of the cylindrical cavity BPM with $4.76\,$GHz resonance frequency can be found in [10]. First measurements have been made with 4 BPMs placed between the undulators. The electronics was build without I-Q demodulator. Therefore phase drifts for different machine conditions and beam angle and bunch tilt influences the resolution measurement. The resolution between 1.7 and $5.2\,\mu$m was obtained [10].

A new circuit has been realized with an I-Q demodulation, applying the homodyne method and the beamline was rearranged with only drifts between 3 BPMs. With this configuration the resolution improved to $0.2\,\mu$m [11].

Re-entrant Cavity BPM for the European XFEL

Cylindrical re-entrant cavity BPM built at Saclay with dipole mode resonance frequency of $1.724\,$GHz will be used in the cold accelerator at cryogenic temperature. The design is realized without slots, therefore the monopole mode at $1.255\,$GHz is filtered with hybrids, as described in details in ref. [12]. A single down conversion per plane is used, applying the homodyne method. The charge calibration is made by using the sum signal from the hybrid, corresponding to the monopole mode. Measurements at FLASH show a resolution of 4 and 8 μm, the difference is caused by different low-pass filters [12, 13]. This results fulfills the requirement for the resolution of $50\,\mu$m.

Undulator Cavity BPM for the European XFEL

The design of the cavity BPM is based on [10] adapted to the requirements of the European XFEL: smaller beam pipe ($10\,$mm diameter) and a lower resonance frequency of $3.3\,$GHz. Few prototypes already produced at DESY, one is installed at FLASH. The measured frequency, loaded quality factor and sensitivity are in agreement with the prediction. An improvement of the orthogonal coupling has been done, see [9]. Next step is to include 3 BPM in FLASH with electronics to measure the resolution.

Linac Coherent Light Source Cavity BPM

The cylindrical cavity BPMs were developed at the Argonne National Laboratory with a dipole mode resonance

frequency of 11.384 GHz to be used between the undulators at LCLS. The detail of the design can be found in ref. [14]. The fields of the cavities are transmitted with waveguides to the receiver, below the undulator girder. The receiver uses a single-stage heterodyne method, as described in [15]. Measurements at the Advanced Photon Source low energy undulator test line result in resolution between 0.26 and 0.32 μm [16]. Meanwhile 33 cavity BPMs are used for the resolution measurements at LCLS with the cross correlation method. The median resolution of all BPMs is 0.44 μm for the horizontal, and 0.23 μm for the vertical plane, as described in ref. [17].

ILC Spectrometer With Cavity BPM

A prototype of an ILC spectrometer using cylindrical cavity BPMs as described in ref. [18] is installed at the SLAC end station A. The design is presented in [19] and provides a resonance frequency of about 2.9 GHz. The electronics consists of a I-Q demodulation with Heterodyne method, a single stage down-conversion is used. The middle BPM (of three) is mounted on a dual axis mover system. The BPMs vibrational motion of the horizontal plane is monitored by an interferometer system. It was shown that the non-rigid motion for the middle BPM is 620 nm, for the other two it is below 100 nm. Therefore by measuring the BPM resolution and assuming all three have the same behavior the non-rigid motion dominates the result. The measured resolution is about 0.5 μm [1] which fulfills the requirement.

Cavity BPM for the ILC Interaction Point

To control the interaction of the beam collisions the resolution of the BPM has to be few nanometers. Some iterations are made to improve the resolution. Cylindrical cavity BPMs are tested with a special metrology system to stabilize the non-rigid motion, which leads to the resolution of 15 nm [20] at the KEK Advanced test facility. The next tested prototype was a rectangular design for each transverse plane to suppress the orthogonal coupling. These prototypes were fixed on a heavy granite table. The steerers available for the calibration produce a certain offset. This system uses a hybrid to increase the weak amplitude and a homodyne method is applied for the I-Q demodulation. The resolution of $(8.72 \pm 0.28(\text{stat.}) \pm 0.35(\text{syst.}))$ nm was measured [21].

SUMMARY

The basic principles of the cavity BPM designs are presented. The influence of the beam angle and bunch tilt are discussed and the rejection of the monopole mode is described. An overview of the signal processing is shown and the main influence on the resolution is discussed. The examples from different institutes have shown that the cavity BPMs are able to provide resolutions at a few nanometer level.

02 BPMs and Beam Stability

REFERENCES

[1] M. Slater *et al.*, "Cavity BPM system tests for the ILC energy spectrometer", NIM A 592, 201-217, 2008.

[2] W. C. Barry, "Broad-Band characteristics of circular button pickups", Proceedings at the Accelerator Instrumentation Workshop, 1992.

[3] T. Suwada *et al.*, "Stripline-type beam-position monitor system for single-bunch electron-positron beams", NIM A 440, 307-319, 2000.

[4] M. Abramowitz and I. A. Stegun, "Handbook of Mathematical Functions", Dover Publications, Inc., New York, 1965.

[5] Computer Simulation Technology (CST), http://www.cst.com.

[6] S. Walston *et al.*, "Performance of a high resolution cavity beam position monitor system", SLAC-PUB-12492, 2007.

[7] V. Balakin *et al.*, "Experimental results from a microwave cavity beam position monitor", Proceedings PAC, 1999.

[8] V. Vogel *et al.*, "Performance of a nanometer resolution beam position monitor system", UCRL-CONF-216283, Nanobeam 2005.

[9] D. Lipka *et al.*, "Orthogonal coupling in cavity BPM with slots", These proceedings: MOPD02, 2009.

[10] H. Maesaka *et al.*, "Beam position monitor at the SCSS prototype accelerator", Proceedings APAC, 2007.

[11] H. Maesaka *et al.*, These proceedings: MOPD07, 2009.

[12] C. Simon *et al.*, "Beam position monitors using a Re-entrant cavity", Proceedings DIPAC, 2007.

[13] C. Simon *et al.*, "Performance of a reentrant cavity beam position monitor", Physical Review AB 11, 082802, 2008.

[14] G. Waldschmidt *et al.*, "Electromagnetic design of the rf cavity beam position monitor for the LCLS", Proceedings PAC, 2007.

[15] R. Lill *et al.*, "Design and performance of the LCLS cavity BPM system", Proceedings PAC, 2007.

[16] R. Lill, private communication, 2009.

[17] S. Smith, "LCLS Cavity BPM", These proceedings: TUOC03, 2009.

[18] A. Lyapin *et al.*, "A prototype energy spectrometer for the ILC at end station A in SLAC", Proceedings PAC, 2007.

[19] A. Lyapin *et al.*, "A prototype S-band BPM system for the ILC energy spectrometer", EUROTeV-Report-2008-072, 2009.

[20] S. Walston *et al.*, "Resolution of a high performance cavity beam position monitor system", Proceedings PAC, 2007.

[21] Y. Honda *et al.*, "Development of a high-resolution cavity-beam position monitor", Physical Review AB 11, 062801, 2008.